Supporting Information

Anisotropic Plasmonic CuS Nanocrystals as Natural Electronic Material with Hyperbolic Optical Dispersion

R. Margoth Córdova-Castro[‡]**, Marianna Casavola*[‡]*, Mark van Schilfgaarde, Alexey V. Krasavin, Mark A. Green, David Richards, and Anatoly V. Zayats*

Department of Physics and London Centre for Nanotechnology, King's College London, London WC2R 2LS, United Kingdom

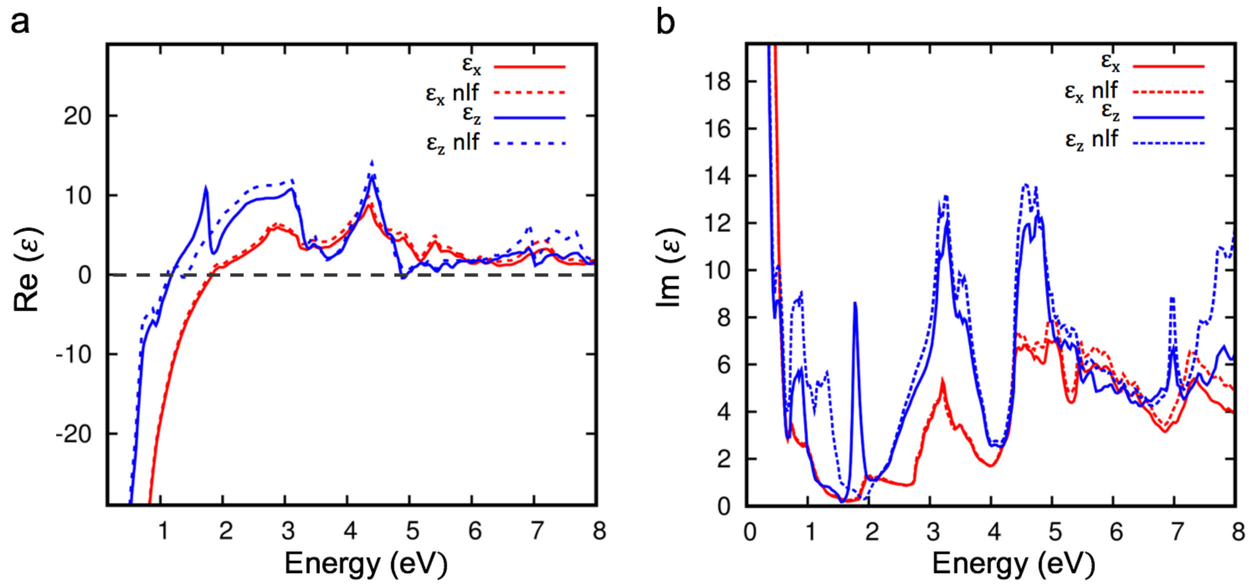

Figure S1. Longitudinal components ε_x=ε_y and ε_z of the (a) real and (b) imaginary parts of the dielectric function, with (dashed lines) and without (solid lines) local field corrections.

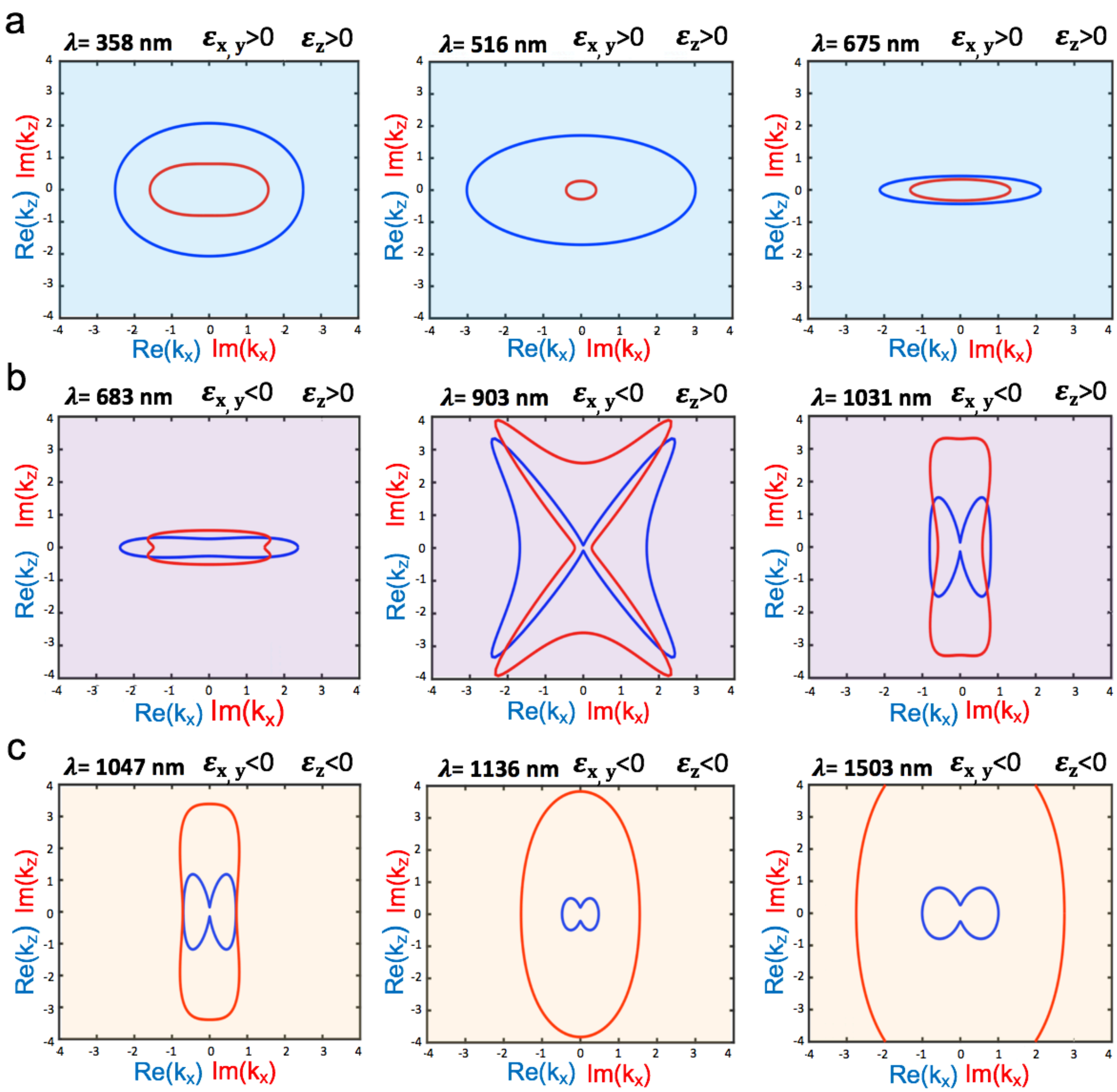

Figure S2. Isofrequency curves for (blue) [Re{$k_x(\omega)$},Re{$k_y(\omega)$}=0, Re{$k_z(\omega)$}], refractive index related, and (red) [Im{$k_x(\omega)$}, Im{$k_y(\omega)$}=0, Im{$k_z(\omega)$}], absorption related, parts of the wavevector for the TM electromagnetic waves with the electric field component in z-direction in bulk anisotropic CuS for the vacuum wavelengths $\lambda = 2\pi/\omega$ in different dispersion regimes: (c) elliptic (anisotropic dielectric), (d) hyperbolic and (e) anisotropic plasmonic.

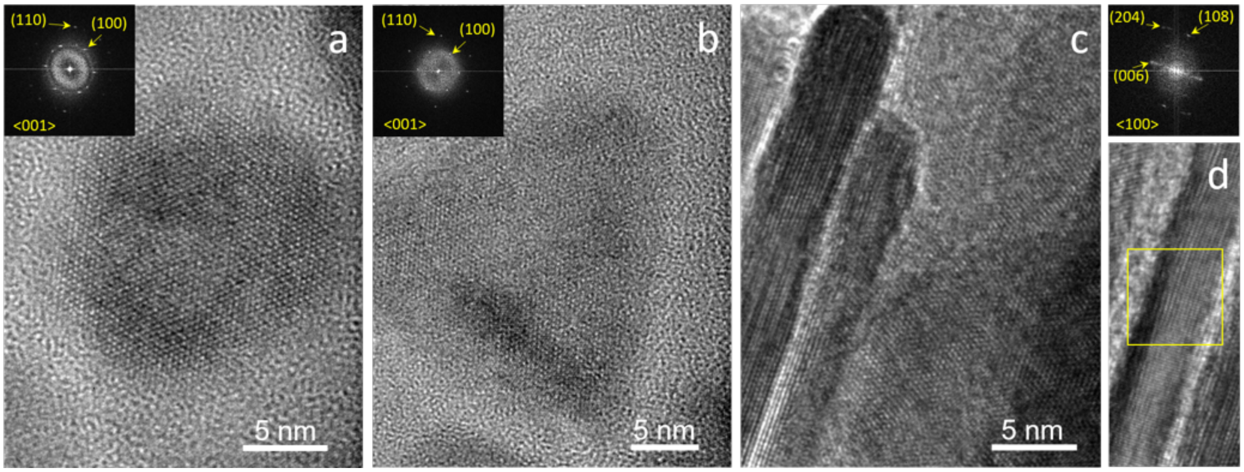

Figure S3. (a-c) HRTEM micrograph of (a) a CuS NC of a 16 nm lateral size with a circular shape in the <001> zone axis; (b) a CuS NC of a 24 nm lateral size with quasi-triangular shape in the <001> zone axis, (c-d) CuS NCs of a 127 nm lateral size lying flat (a,b) and vertically oriented (c,d) on the substrate. The insets show the fast Fourier transform (FFT) of the corresponding micrographs.

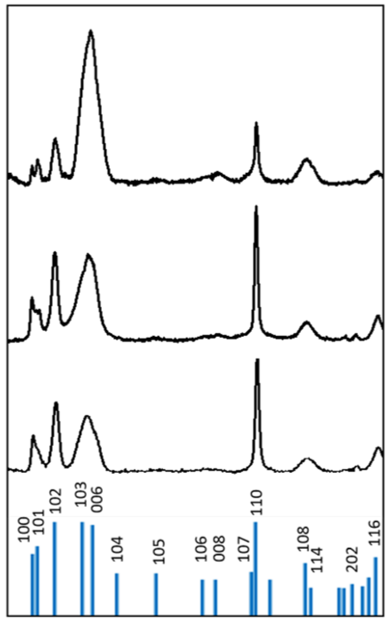

Figure S4. X-Ray Diffraction (XRD) patterns of CuS NCs of (from bottom to top) 16, 24, and a 56 nm lateral sizes. For comparison a standard XRD pattern of covellite CuS (reference: CuS #01-075-2233) is plotted in blue.

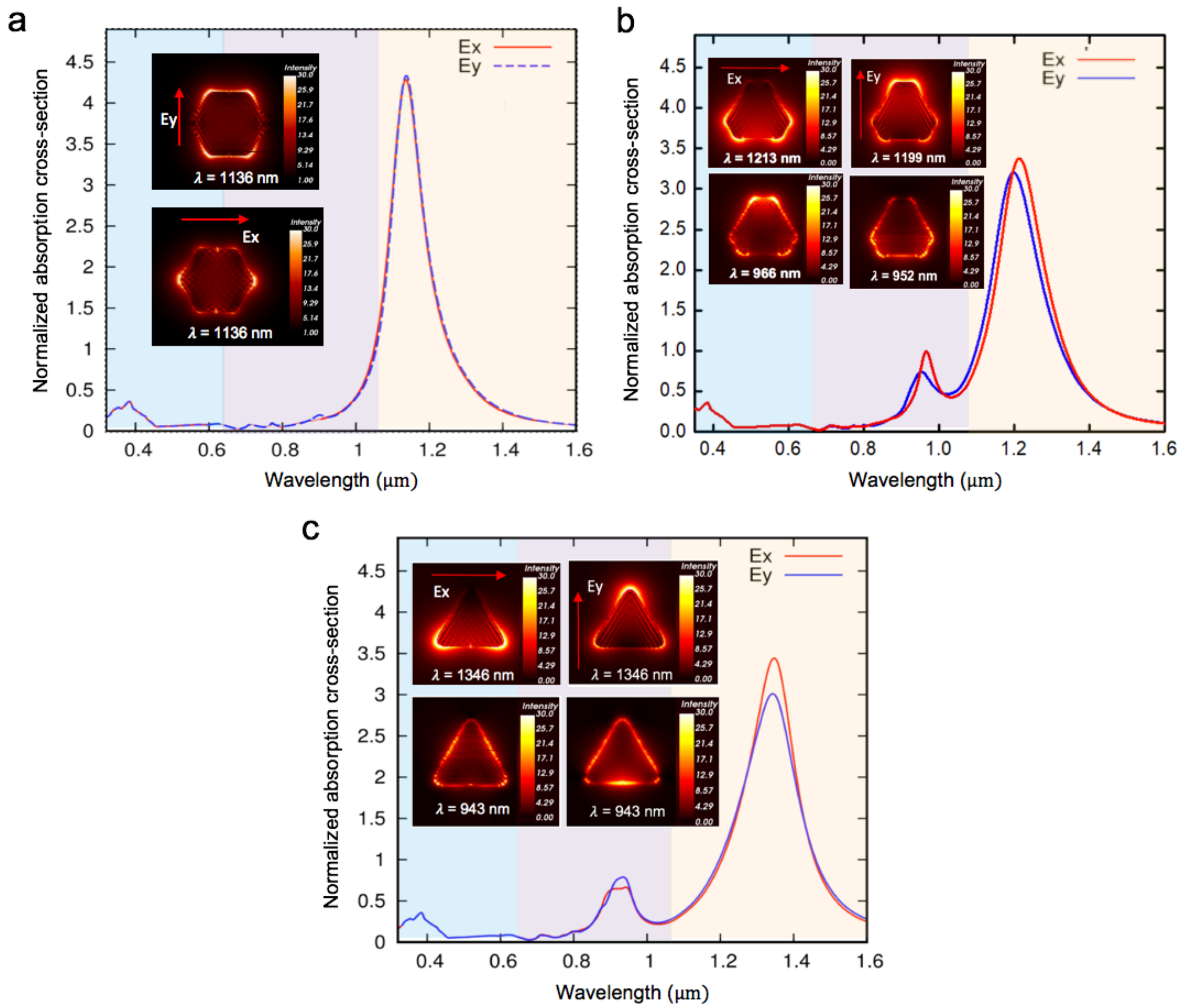

Figure S5. Calculated spectra of normalized absorption cross-sections for (a) hexagonal (b) hexa-triangular and (c) triangular shapes (upon illumination with a linearly polarized plane wave with the electric field along *x* and *z* axis, respectively. Near-field intensity maps are shown at the corresponding resonant wavelengths for each direction.

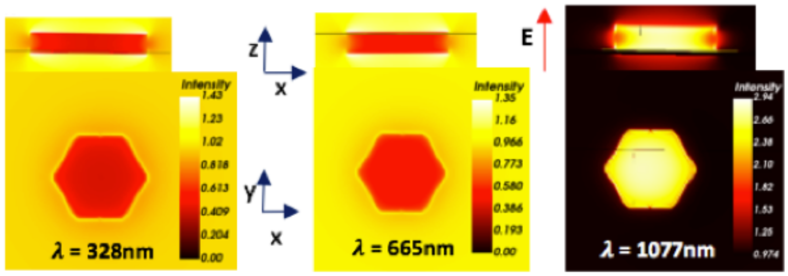

Figure S6. Near-field intensity maps for the CuS NC of a hexagonal shape of a 19 nm lateral size and a 5 nm thickness surrounded by a medium with a refractive index of 1.45, calculated at the spectral absorption peaks (Fig. 4b) for out-of-plane polarized illumination.

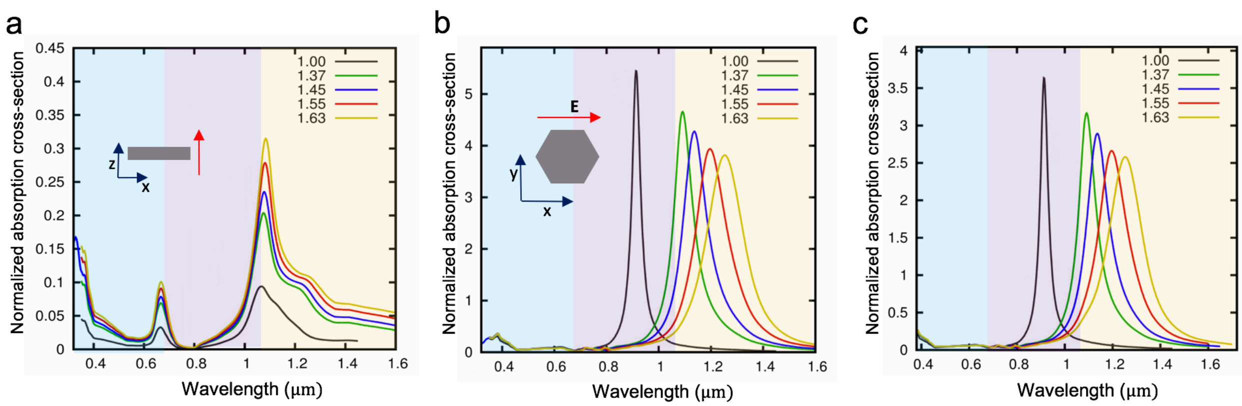

Figure S7. Calculated spectra of normalized absorption cross-sections for isolated CuS nanocrystals of a hexagonal shape surrounded by various dielectric media and illuminated with a linearly polarized plane wave with the electric field along (a) z axis (b) x axis and (c) average of the field along x, y, and z axes with the corresponding anisotropic dielectric function for each axis.

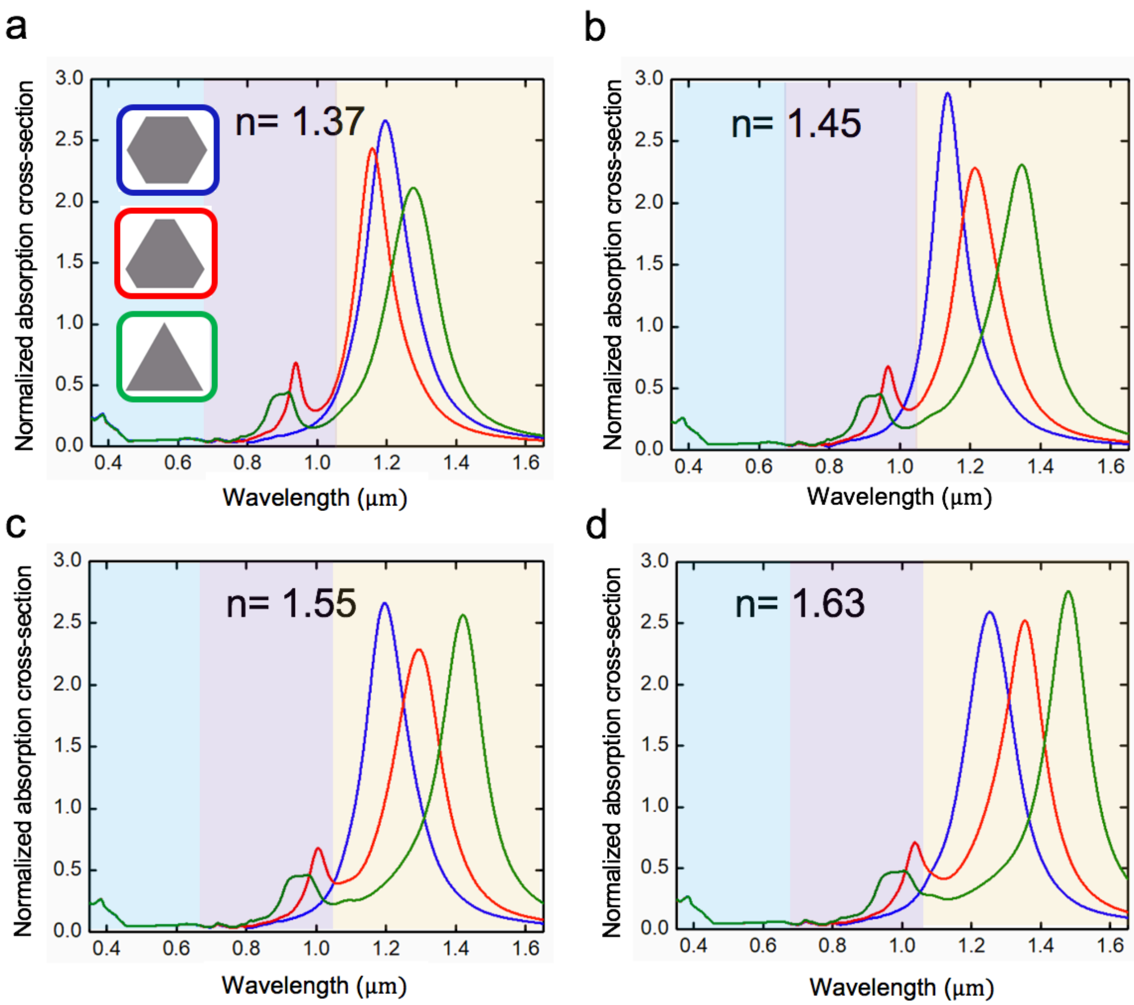

Figure S8. Calculated spectra of normalized absorption cross-sections for CuS nanocrystals of a hexagonal, triangular and hexa-triangular shapes (19 nm lateral size and 5 nm thickness) surrounded different refractive index media as indicated in the panels. The spectra are averaged over random NC orientations with respect to the linearly polarised incident light.

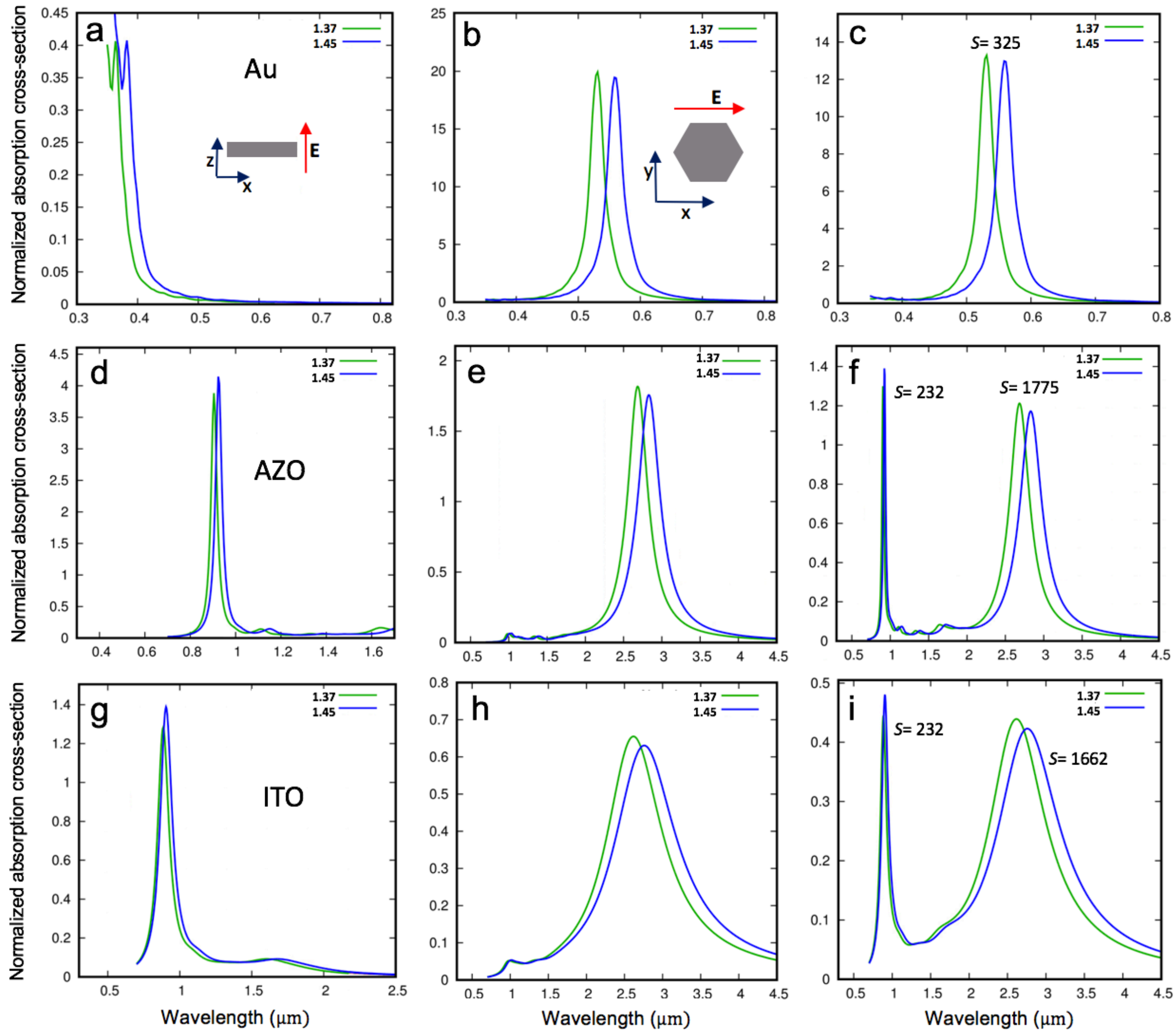

Figure S9. Calculated spectra of normalized absorption cross-sections for hexagonal nanoparticles (19 nm size and 5 nm thickness) dispersed in solvents with refractive indices of 1.37 and 1.45 for (a-c) Au, (d-f) AZO an (g-i) ITO: (a,d,g) and (b,e,h) light polarization normal and in-plane of the nanoparticles, respectively, (c,f,i) average response of randomly oriented nanoparticles.

Fitting approach based on the Drude-Sommerfeld model.

In previously reported studies,[14,26-30] the complex dielectric function of CuS nanocrystals was calculated using the Drude-Sommerfeld model

$$\varepsilon(\omega) = \varepsilon_{\infty} - \omega_p^2/(\omega^2 + i\gamma\omega), \tag{4}$$

where ε_{∞} takes into account the polarization background of the ion cores, γ is the damping constant and ω_p is the Drude plasma frequency. These studies solved an inverse problem by taking the experimental values for the width of the resonance absorption curve to determine γ, and the maximum of the absorption peak in the measured absorption spectral curve to determine the frequency of the localized surface plasmon resonance ω_{LSP}. The plasma frequency ω_p (defined by Eq. 4) is then evaluated from the real part of the Drude-Sommerfeld permittivity $\mathrm{Re}\{\varepsilon(\omega_{LSP})\} = 1 - \omega_p^2/(\omega_{LSP}{}^2 + \gamma^2)$ and the analytical solution, averaged over nanoparticle orientations, corresponding to the resonant conditions of an oblate spheroid $\mathrm{Re}\{\varepsilon(\omega_{LSP})\} = \varepsilon_m[(L_j - 1)/L_j]$ for j=1,2,3, where L_j is the geometrical factor of the spheroid and ε_m is the permittivity of the surrounding medium.

We also follow this approach to show that this procedure will produce calculated absorption spectra very similar to the experimental measurements, as expected since the parameters were derived from the experimental curves. Nevertheless, the permittivity derived following this approach is incorrect even if a match with the experimental extinction spectra is obtained. For example, for the experimental extinction curve with $\omega_{LSP} = 1.13$ eV, observed for CuS NCs immersed in a medium of 1.45 refractive index (Figure 4a), and taking into account ε_{∞}=1 and $\varepsilon_m = 1.8769$ in the analytical solution for the resonant condition of an oblate spheroid with aspect ratio of $h = (a/c) = 3.8$, $L_1 = L_2 = 0.154$ and $L_3 = 1 - 2(L_1) = 0.6921$, we obtain $\omega_p = 4.01$ eV and the damping constant $\gamma = 0.39$ eV. Figure S10 shows the comparison of the absorption spectral curve of CuS NCs calculated using the complex dielectric function determined with the Drude-Sommerfeld approach and using the complex dielectric function calculated from first principles using QSGW and RPA. One can see that, in the former case the two free fitting parameters, ω_p and γ, must be changed to obtain agreement for different refractive indices of surroundings and do not correctly describe properties of the material away from the LSP resonance or the polarization properties of individual NCs. In particular, the Drude-Sommerfeld approach does not correctly describe the sensitivity of the CuS LSP resonance on the solvent's refractive index and the NC size. On the other hand, the use of permittivity evaluated from the *ab initio* band structure allows the correct prediction of the frequency of LSPs, and its refractive index dependences, without any fitting parameters, while the deviations in the width of the resonances is considered to be related to the dispersion of the nanocrystal shape and size. The use of the fitting within the Drude formalism might have been justifiable for a NC made from an isotropic material, but completely breaks down for anisotropic materials such as CuS.

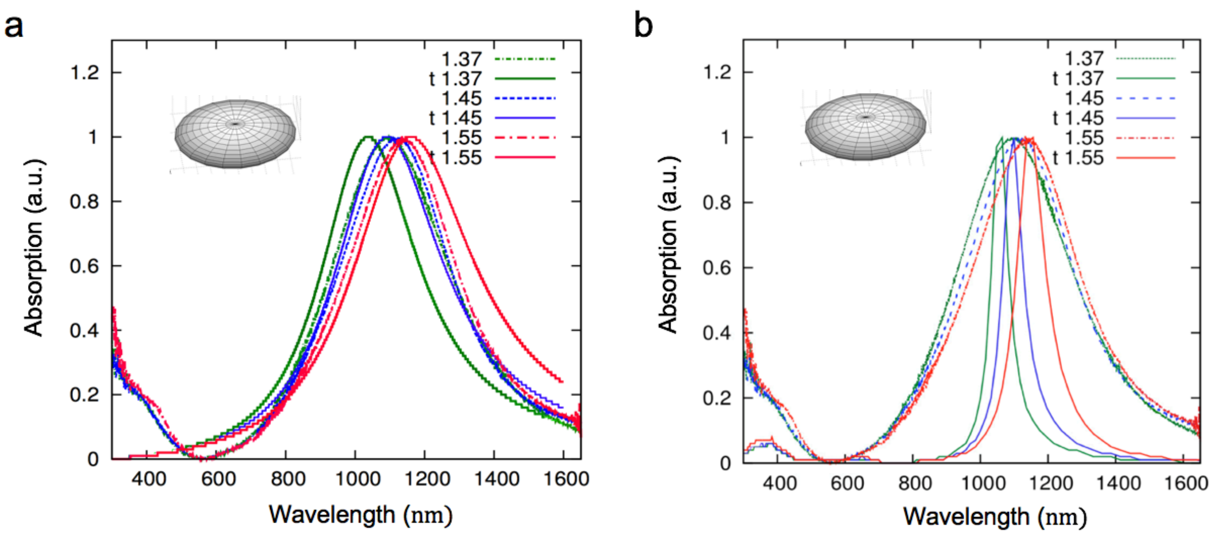

Figure S10. (a) Experimental (dashed/dotted lines) and theoretically fitted (t, solid lines) normalized absorption spectra for an isolated oblate spheroid using the Drude model for the NC permittivity: the plasma frequency and damping coefficient are used as fitting parameters. The refractive indeces of surroundings for different curves are indicated in the legends. (b) Same as (a) but for the anisotropic permittivity obtained from the *ab initio* calculations. A random orientation of the spheroidal particles is assumed in both (a) and (b).